ЯДЕРНА ФІЗИКА
NUCLEAR PHYSICS

УДК 539.125.17+539.126.17 https://doi.org/10.15407/jnpae2026.01.016

Ya. D. Krivenko-Emetov[1,2,3,*], B. I. Sydorenko[2,a]

[1] *National Technical University of Ukraine "Igor Sikorsky Kyiv Polytechnic Institute", Kyiv, Ukraine*
[2] *Institute for Nuclear Research, National Academy of Sciences of Ukraine, Kyiv, Ukraine*
[3] *Taras Shevchenko National University of Kyiv, Kyiv, Ukraine*

*Corresponding author: y.kryvenko-emetov@kpi.ua; krivemet@ukr.net

INCLUSION OF THE LONGITUDINAL COMPONENT OF THE TRANSFERRED MOMENTUM Q_z AND THE TRANSVERSE RELATIVE MOMENTUM $\mathbf{p}_\perp$ IN THE DIFFRACTION APPROACH TO THE $H(d, p)X$ REACTIONS[b]

In this work, within the framework of the Glauber - Sitenko approximation, we present an analysis of the differential cross section for deuteron breakup with proton emission in the reaction $H(d, p)X$ at small proton emission angles ($\theta_p < 7$ μrad). The study employs several parameterizations of the deuteron wave function, including the single-Gaussian, the multi-Gaussian K2 parameterization, and models based on the Av18 and Nijm I nucleon-nucleon potentials.

Particular attention is paid to the effects of small longitudinal components of the transferred momentum ($|Q_z| \le 0.5$ GeV/c in the laboratory frame) and the transverse momentum of the proton-neutron pair $\left(\mathbf{p}_\perp = (p_x, 0) \le 0.5\,\text{GeV/c}\right)$ in the antilaboratory reference frame. The results are compared with available experimental data, especially in the region of longitudinal momenta $k_z = p_3^* = 0.25 - 0.5$ GeV/c (in the antilaboratory frame), where quark effects are expected to become significant. Calculations show an increase in the differential cross section with increasing transverse momentum, as well as a small shift – and a noticeable enhancement – of the cross-section maximum when the longitudinal component Q_z is included.

Keywords: deuteron, diffractive breakup, relativistic effects, quark structure, differential cross section, Glauber - Sitenko approach, longitudinal momentum, transverse momentum, dibaryon, $d^*(2380)$.

1. Introduction

The deuteron, being the simplest bound system of nucleons, continues to serve as one of the key subjects of investigation in nuclear physics, particularly for understanding the non-central nature of nuclear forces, as well as exchange, relativistic, and short-range quark-gluon effects. Despite significant progress in the theoretical description of the deuteron, aspects such as its relativistic dynamics and behavior at high momentum transfers remain insufficiently explored. These issues are closely linked to fundamental problems in the theory of strong interactions, especially to the application of quantum chromodynamics (QCD) to few- and many-body nuclear systems (for details, see, e.g., [1–6]).

One of the most promising approaches to studying deuteron structure is through the analysis of its high-energy breakup reactions on nuclear targets, particularly inclusive processes such as $A(d, p)X$-type reactions. Experiments carried out at momenta of about 2.1 - 10.8 GeV/c [7–16] have revealed significant discrepancies between experimental data (including differential cross sections, tensor analyzing power T_{20}, and polarization transfer observables) and the predictions of traditional models based on the impulse approximation.

These discrepancies, as demonstrated in several studies, underscore the necessity of accounting for short-range quark structure the deuteron [3, 7, 14, 17–19] and for the role of intermediate dilepton contributions [20–22].

Despite the success of quark-based models in describing the deuteron structure in hard processes, several open questions remain for (d, p) breakup reactions. Experimental studies [7, 9, 12–17, 23, 24] were performed at small proton emission angles ($\theta_p < 7$ μrad), corresponding to the applicability conditions of the Glauber - Sitenko multiple diffraction scattering theory [25–27] (also known as MSDT). This framework, among other results, predicts that Coulomb interaction effects can noticeably influence the $A(d, p)X$ cross section [28–31].

[a] Institute for Nuclear Research, National Academy of Sciences of Ukraine, Kyiv, Ukraine (retired).
[b] Presented at the XXXII Annual Scientific Conference of the Institute for Nuclear Research of the National Academy of Sciences of Ukraine, Kyiv, May 26–30, 2025.

Glauber - Sitenko multiple diffraction scattering theory [25–27] (also known as MSDT). This framework, among other results, predicts that Coulomb interaction effects can noticeably influence the $A(d, p)X$ cross section [28–31].

Beyond the Coulomb contribution, unresolved issues within MSDT include the role of the longitudinal transferred momentum component Q_z (see, e.g., [32, 33]) – neglected in classical diffraction theory [25, 26] – and the transverse momenta of the proton-neutron pair $\mathbf{p}_\perp$ in the antilaboratory frame [34, 35]. Several studies [31, 32, 34] have shown that ignoring these effects in standard MSDT may lead to misinterpretation of experimental data.

In this work, we analyze the $H(d, p)X$ reaction, taking into account both the longitudinal transfer Q_z and the transverse nucleon momenta $\mathbf{p}_\perp$ in the antilaboratory frame. Using different nucleon-nucleon potentials, particularly the Nijmegen (Nijm I) potential [36], we examine their influence on the differential cross section and compare the results with experiment. Special attention is paid to the region of large relative momenta ($k_z \geq 250$ MeV/c, in the antilaboratory frame), where conventional models show marked discrepancies with the data [7, 9, 11, 14].

The objectives of this study are:

1. To include Q_z in the laboratory frame and transverse nucleon momenta $\mathbf{p}_\perp$ in and analyze their effect on the cross-section shape.

2. To assess how these factors influence previous conclusions regarding the manifestation of quark degrees of freedom in the short-range part of the deuteron wave function.

The second point of the stated objective deserves separate discussion. The relevance of this study is emphasized by the fact that, soon after the pioneering works [7, 18], where the observed rise of the invariant cross section in the antilaboratory frame (300 - 500 MeV/c) was attributed to an S-wave quark component in the deuteron wave function, several alternative explanations were proposed (e.g., [37, 38]) suggesting a pion-rescattering origin. However, this interpretation raises doubts.

The antilaboratory frame in scattering problems is analogous to the s-channel: the position of maxima in the differential cross section can indicate the mass of intermediate exchange particles, as in the relativistic Breit - Wigner resonance description. If the pions mentioned were on-shell, their energies would be below the characteristic 300 - 500 MeV range.

Moreover, studies of quark behavior in the nuclear medium show that the effective masses of light quarks (u, d, s) increase to 300 - 500 MeV/c^2 [39], which qualitatively contradicts the pion-dominant explanation ($m_\pi \approx 135$ - 140 MeV/c^2).

In addition, several works [22] have shown that nucleon-nucleon collisions with a total energy of about 2380 MeV can produce a six-quark dibaryon resonance $d^*(2380)$. ubtracting the deuteron mass (1876 MeV/c²) yields an excess energy of approximately 0.5 GeV – consistent with the region of the observed enhancement. The first lattice-QCD simulation addressing the possible existence of $d^*(2380)$ was reported by the HAL QCD Collaboration [40].

Although these arguments are mostly qualitative, they support the hypothesis of a quark origin of the enhancement and motivate further investigation. The MSDT framework naturally includes mesonic degrees of freedom – explicitly, through realistic NN potentials (e.g., Nijm I based on meson exchange), and implicitly, via the profile-function parameters. The observed enhancement lies within the MSDT applicability domain, making it a useful tool for testing the quark-based interpretation.

2. General formalism

As is well known [25–27], the diffraction approximation applies when the incident particle's velocity is sufficiently high that the internal structure of the target nucleus remains essentially unchanged during interaction. Under these conditions, the nucleon internal dynamics can be neglected, and the process may be described by a small transferred momentum $\mathbf{Q} = (\mathbf{Q}_\perp, Q_z)$, $|\mathbf{Q}| << |\mathbf{P}|$, where $\mathbf{P}$ is the incident momentum.

This assumption implies both a small scattering angle and a small energy transfer. Since high-energy scattering predominantly occurs at small angles, this kinematic regime is of particular importance. In this limit, $|\mathbf{Q}| << |\mathbf{P}|$ and the vector $\mathbf{Q}$ can be treated as orthogonal to $\mathbf{P}$, i.e., lying in the xy plane [41].

In the standard diffraction theory of composite-nucleus interactions, each deuteron nucleon is assumed to scatter on the target center with a phase shift determined solely by the transverse momentum transfer – an assumption valid for elastic scattering at small angles.

In inelastic deuteron breakup, however, a nucleon may gain not only transverse but also longitudinal momentum Q_z, e.g., when one nucleon is slowed by nuclear forces while the other continues forward, effectively "tearing" the deuteron apart. This effect is absent in the standard MSDT and in the elastic profile function.

It can, however, be incorporated by extending MSDT to include small longitudinal momenta in the transition form factors and inelastic terms in the profile function. As shown in [32, 33, 42], accounting for the longitudinal component can notably affect theoretical predictions.

We consider the general Glauber - Sitenko formalism for the deuteron breakup reaction $H(d, p)$ in the regime of longitudinal proton momentum $p_3 \sim p_d / 2$ (lab frame) and small transverse momentum $\mathbf{p}_\perp$, where the deuteron momentum equals that of the incident particle **P**. In this case, inelastic scattering naturally appears as a modification of the elastic term.

Although the Coulomb interaction is important for the precise reproduction of experimental features, in the specific $H(d, p)$ breakup process, it involves only the two protons (neglecting the neutron's electric form factor) and can therefore be ignored in the first approximation.

Neglecting the Coulomb interaction, the strong-interaction amplitude of deuteron breakup $F_{\text{str.}}(\mathbf{p}_\perp, p_3, \mathbf{Q})$ takes the form:

$$F_{str}(\mathbf{p}_\perp, p_3, \mathbf{Q}) =$$

$$= \frac{ip_d}{2\pi}\int d^2\mathbf{B} e^{i\mathbf{Q}_\perp\cdot\mathbf{B}}\int d^3\mathbf{r}\psi_{\mathbf{k}}^{*(-)}(\mathbf{r})(1-S(\mathbf{B},\mathbf{r}))\psi_0(\mathbf{r}), \quad (1)$$

where $\psi_0(\mathbf{r})$ is the deuteron wave function, $\psi_{\mathbf{k}}^{*(-)}(\mathbf{r})$ is the distorted final-state wave function of the ***pn***-pair, and $S(\mathbf{B}, \mathbf{r})$ is the Glauber - Sitenko scattering operator; here $\mathbf{p}_\perp$ and p_3 denote the transverse and longitudinal proton momentum components, $\mathbf{Q} = (\mathbf{Q}_\perp, Q_z)$ is the momentum transfer, $\mathbf{B} = \mathbf{b}_p + \mathbf{b}_n$ the average impact parameter, $\mathbf{r}_\parallel = r_z$ the longitudinal component of $\mathbf{r} = \mathbf{r_p} - \mathbf{r_n}$.

The relative momentum (non-relativistic) is $\mathbf{k} = \left(\mathbf{p}_\perp - \frac{1}{2}\mathbf{Q}_\perp, p_3\right)$, for relativistic (in antilaboratory frame, $p_3^* + n_3^* = 0$): $\mathbf{k}_\perp = \mathbf{p}_\perp - \frac{1}{2}\mathbf{Q}_\perp$, $k_3 = k_z = p_3^*$.

Within the optical approximation:

$$S(\mathbf{B},\mathbf{r}) = 1 - \Gamma_1\left(\mathbf{B} + \frac{1}{2}\mathbf{r}_\perp\right) - \Gamma_2\left(\mathbf{B} - \frac{1}{2}\mathbf{r}_\perp\right) +$$

$$+\Gamma_1\left(\mathbf{B} + \frac{1}{2}\mathbf{r}_\perp\right)\Gamma_1\left(\mathbf{B} - \frac{1}{2}\mathbf{r}_\perp\right), \quad (2)$$

where $\mathbf{r}_\perp$ is the projection onto the *xy*-plane, and Γ_1, Γ_2 are profile functions of deuteron nucleons.

Using $\mathbf{B} = \mathbf{b}_p - \frac{1}{2}\mathbf{r}_\perp = \mathbf{b}_n + \frac{1}{2}\mathbf{r}_\perp$ the amplitude decomposes as:

$$F_{str}(\mathbf{p}_\perp, p_3, \mathbf{Q}) =$$

$$= \frac{ip_d}{2\pi}\int d^2\mathbf{B}\ e^{i\mathbf{Q}_\perp\cdot\mathbf{B}}\int d^3\mathbf{r}\psi_{\mathbf{k}}^{*(-)}(\mathbf{r})\Big[\Gamma\left(\mathbf{b}_n, Q_z, \mathbf{r}_\parallel\right) + \Gamma\left(\mathbf{b}_p, Q_z, \mathbf{r}_\parallel\right) - \Gamma\left(\mathbf{b}_n, Q_z, \mathbf{r}_\parallel\right)\Gamma\left(\mathbf{b}_p, Q_z, \mathbf{r}_\parallel\right)\Big]\psi_0(\mathbf{r}) =$$

$$= F_{str}^{n}(\mathbf{p}_\perp, p_3, \mathbf{Q}) + F_{str}^{p}(\mathbf{p}_\perp, p_3, \mathbf{Q}) + F_{str}^{np}(\mathbf{p}_\perp, p_3, \mathbf{Q}). \quad (3)$$

Here we have selected the inelastic scattering profile functions accounting for the longitudinal momentum component Q_z in the most general form, including both linear and quadratic terms in the exponential argument (see [32, 33]), as follows $(N = n, p)$:

$$\Gamma(\mathbf{b}_N, Q_z, \mathbf{r}_z) = \frac{e^{(-1)^{\delta_{N,p}} i\cdot\frac{Q_z\cdot r_z}{2}}}{2\pi\cdot i\cdot p_N}\int d^2\mathbf{l}\cdot e^{-i\mathbf{l}\cdot\mathbf{b}_N} f_N(\mathbf{l}) = \frac{(1-i\rho_N)\sigma_N}{4\pi\cdot\beta_N^2}\exp\left\{i\cdot(-1)^{\delta_{N,p}}\cdot\frac{1}{2}Q_z\cdot r_z - \frac{1}{2}\left(\frac{\mathbf{b}_N^2}{\beta_N^2} + \alpha\cdot\beta_N^2\cdot Q_z^2\right)\right\}, \quad (4)$$

where the amplitude of nucleon scattering on the nucleus takes the form:

$$f_N(\mathbf{l}) = \frac{(1-i\rho_N)p_N\sigma_N}{4\pi}\exp\left(-\frac{1}{2}\beta_N^2(l^2 + \alpha\cdot Q_z^2)\right),$$

$$l^2 = \mathbf{l}^2, \quad (5)$$

where σ_N is the total nucleon-proton scattering cross-section, and ρ_N is the ratio of the real to imaginary parts of the amplitude. According to the optical theorem, at the considered energies, the ρ_N parameter is small, while the cross-sections, following Pomeranchuk's theorem, differ only slightly. Therefore, if – as both theory and experiment suggest – $\sigma_p \approx \sigma_n$, we will subsequently use the following natural approximation $\sigma_p \cong \sigma_n \equiv \sigma$ and $\rho_N \ll 1$.

In the profile function, the parameter α is dimensionless and characterizes the ratio of the longitudinal and transverse nuclear scales $\alpha \sim \frac{L_z^2}{b_N^2}$. The parameter b_N defines the characteristic transverse spatial scale (Gaussian width in coordinate space) of the nucleon-nucleon interaction, while $\beta_N \sim 1/b_N$ sets the corresponding scale in momentum space.

For the deuteron with $L_z \sim 1$ - 2 fm and $b_N \sim 1$ - 3 fm, one obtains $\alpha \sim$ O(1). The term $\alpha \cdot \beta_N^2 Q_z^2$ describes the longitudinal breakup of the deuteron along Q_z, whereas $\frac{b_N^2}{\beta_N^2}$ determines its transverse structure. Therefore, when $\alpha \cdot \beta_N^2 Q_z^2 \ll \frac{b_N^2}{\beta_N^2}$ the longitudinal term can be neglected. Substituting typical nuclear scales $\beta_N \sim 0.2$ - 0.6 GeV gives a practical estimate $|Q_z| \ll \frac{(0.2-0.6)}{\sqrt{\alpha}}$ GeV/c. For $\alpha \sim 1$, a conservative assumption is $|Q_z| \lesssim 0.5$ GeV/c; at larger $|Q_z|$, the longitudinal structure of the deuteron must be taken into account (see, e.g., [33]).

With these considerations, the profile functions in our approximation take the form $(N = n, p)$:

$$\Gamma(\mathbf{b}_N, Q_z, \mathbf{r}_z) \sim \frac{(1-i\rho_N)\sigma_N}{4\pi \cdot \beta_N^2} \exp\left((-1)^{\delta_{N,p}} i \cdot \frac{Q_z r_z}{2} - \frac{1}{2}\frac{\mathbf{b}_N^2}{\beta_N^2} \right). \quad (6)$$

Then, introducing the standard definition for the transferred form factor:

$$G(-\frac{1}{2}\mathbf{Q}, \mathbf{k}) = \int d^3\mathbf{r} \cdot e^{i\cdot\mathbf{Q}\cdot\mathbf{r}/2} \psi_{\mathbf{k}}^{*(-)}(\mathbf{r}) \cdot \psi_0(\mathbf{r}) \quad (7)$$

we obtain the compact expressions [42]:

$$F_{str}^N = \frac{(i+\rho_N)\sigma_N p_d}{4\pi} G((-1)^{\delta_{(N,p)}} \frac{1}{2}\mathbf{Q}, \mathbf{k}) \exp\left(-\frac{1}{2}\beta_N^2 \mathbf{Q}_\perp^2 \right), \quad (8)$$

$$F_{str}^{np} = -\frac{i \cdot p_d}{4\pi p_n p_p} \int d^2\mathbf{l}_p f_p(\mathbf{l}_p) \times$$

$$\times G\left(\frac{1}{2}\mathbf{Q}_\perp - \mathbf{l}_p, \mathbf{k} \right) f_n(\mathbf{Q}_\perp - \mathbf{l}_p). \quad (9)$$

This generalized MSDT formalism thus provides a comprehensive description of both transverse and longitudinal mechanisms in deuteron breakup, essential for accurate theoretical predictions.

3. Wave functions and normalization issues

To draw general conclusions, both analytical and numerical calculations were performed for a broad class of Gaussian-type deuteron wave functions, including the single-Gaussian parametrization [33], multi-Gaussian K2 [43], and realistic AV18 [44] and Nijm I [36] potentials.

As an example, for the Nijm I potential, the *S*- and *D*-wave components are approximated as

$$u(r) = r\sum_{i=1}^{N} A_i e^{-\alpha_i r^2}, \qquad w(r) = r^3 \sum_{i=1}^{N} B_i e^{-\beta_i r^2},$$

and the normalized bound deuteron state i

$$\psi_0(\mathbf{r}) = \sqrt{N_s}\psi_s(\mathbf{r}) + \sqrt{N_d}\psi_d(\mathbf{r}) =$$

$$= \frac{1}{\sqrt{4\pi}r}(u(r) + w(r)),$$

where N_s and N_d are the probabilities of the *S*- and *D*-wave components ($|N_s| + |N_d| = 1$), and ψ_s, ψ_d are normalized and orthogonal: $\int \psi_s^* \psi_s d^3r = 1$, $\int \psi_d^* \psi_d d^3r = 1$, $\int \psi_s^* \psi_d d^3r = 0$.

As is known, for Gaussian wave functions, it is impossible to construct an unbound *pn* state that exactly satisfies orthogonality and completeness [45]. Following [31, 45], the unbound state can be written as

$$\psi_{\mathbf{k}}(\mathbf{r}) = De^{i\cdot\mathbf{r}\cdot\mathbf{k}} - C(\widetilde{\varphi_s}(\mathbf{k})\psi_s(\mathbf{r}) +$$

$$+\widetilde{\varphi_d}(\mathbf{k})\psi_d(\mathbf{r})) \sim De^{i\cdot\mathbf{r}\cdot\mathbf{k}} - C\widetilde{\varphi_s}(\mathbf{k})\psi_s(\mathbf{r}),$$

where $\psi_s(r) = \frac{1}{(4\pi)^{1/2}}\frac{u(r)}{\sqrt{N_s}}$ and $\widetilde{\varphi_s}$ ($\widetilde{\varphi_d}(\mathbf{k})$) are the Fourier transforms of the *S* (*D* – components). For the *S*-wave [33], $\widetilde{\varphi_s}(\mathbf{k}) = \frac{1}{(2\pi)^{3/2}} \int \psi_s^*(\mathbf{r}) \cdot e^{i\cdot\mathbf{k}\cdot\mathbf{r}} d^3r =$

$$= \sqrt{\frac{1}{4\pi}} \sum_{i=1}^{N} \frac{A_i}{(2\alpha_i)^{3/2}} e^{-\frac{k^2}{4\alpha_i}}.$$

Orthogonality to the bound state requires $\int \psi_{\mathbf{k}}^* \psi_s d^3r = 0$, i.e. $C = (2\pi)^{3/2} D$, but in this case, the exact normalization of the continuous spectrum $< \psi_{\mathbf{k}'} | \psi_{\mathbf{k}} >= (2\pi)^3 \delta^{(3)}(\mathbf{k} - \mathbf{k}')$, which cannot be strictly satisfied. This condition is approximately fulfilled when α_i approaches zero; for example, in the single-Gaussian case *D* approaches unity for both non-zero and zero values of $\mathbf{k} - \mathbf{k}'$ (see Appendices B and C in Ref. [42] for details).

4. Comparison with experiment

As shown in the previous section, following the standard MSDT (see, e.g., [29–33, 42, 45]), the wave function can be expressed in terms of the standard two-nucleon deuteron wave functions (in our case K2, AV18, Nijm I), renormalized according to the condition formulated in [31, 42].

The differential invariant cross-section is defined by the formula

$$E_p \frac{d^3\sigma}{d^3k} =$$

$$= E_p \frac{1}{(2\pi)^3} \int d^2\mathbf{Q}_\perp \, |F_{str}(\mathbf{p}_\perp, p_3, \mathbf{Q}_\perp, Q_z)|^2 = E_p^* \frac{d^3\sigma^*}{d^3k^*}, \quad (10)$$

where E_p^* denotes the proton energy in the antilaboratory frame (E_p in the laboratory frame).

Unlike in Ref. [31], we retain both the transverse components of the proton-neutron relative momentum $\mathbf{p}_\perp$ and the longitudinal component of the momentum transfer Q_z, which enables a detailed study of their kinematic contributions to the invariant cross section.

As mentioned above, to obtain more general conclusions, the comparison with the experimental data [7] (1992) and [34] (2019) was carried out for a broad class of deuteron potentials. Since for realistic deuteron potentials even when only the *S*-wave component is taken into account, the invariant cross section acquires an extremely cumbersome analytical form (see [42], Appendix D), we restrict ourselves here to a graphical representation of several characteristic consequences of including Q_z, and $\mathbf{p}_\perp$.

We obtained the following results: for the single-Gaussian parametrization [33] (Figs. 1 and 2); for the multi-Gaussian parametrization K2 [43, 46] (Figs. 3 and 4); for the multi-Gaussian parametrization Av18 [44, 47] (Figs. 5 and 6); and for the realistic Nijm I potential [36, 47] (Fig. 7 and 8).

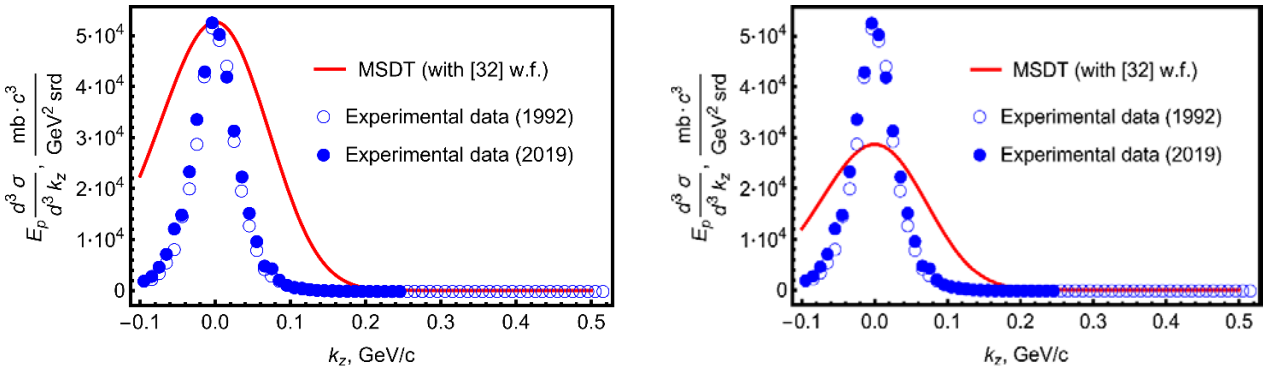

Fig. 1. *a* – Dependence of $E_p \frac{d^3\sigma}{d^3k}$ on k_z, using Gaussian [33] at $p_x = 10^{-5}$ GeV/c and $Q_z = 10^{-5}$ GeV/c. Points – data, curve – MSDT. *b* – The same $E_p \frac{d^3\sigma}{d^3k}$ vs k_z, at p_x = 0.5 GeV/c and Q_z = 10^{-5}GeV/c. (See color Figure on the journal website.)

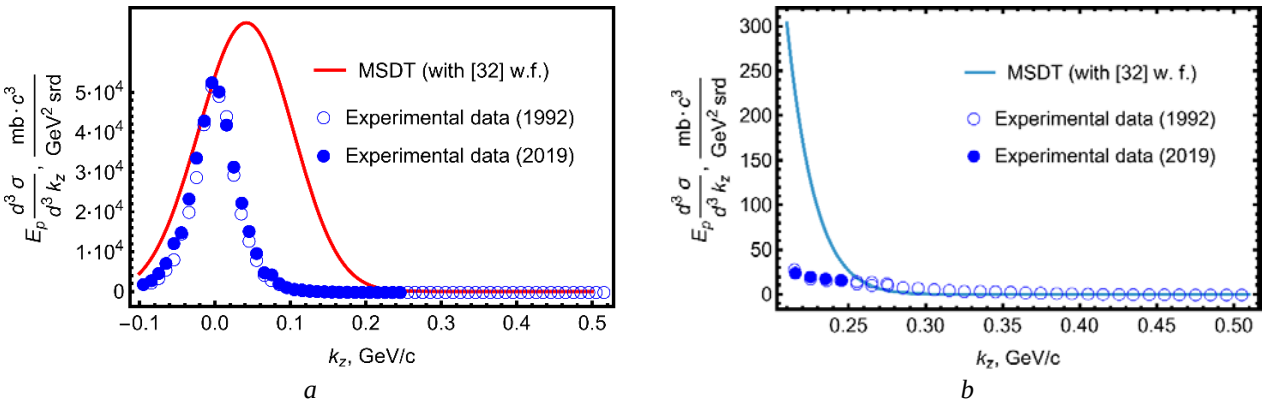

Fig. 2. *a* – The same as Fig. 1 at p_x = 10^{-5}GeV/c and Q_z = 0.5 GeV/c. *b* – Within the MSDT model with Gaussian, dibaryon states with energies above 0.25 GeV/c are not supported ($p_x = 10^{-5}$ GeV/*c*, $Q_z = 10^{-5}$ GeV/*c*). (See color Figure on the journal website.)

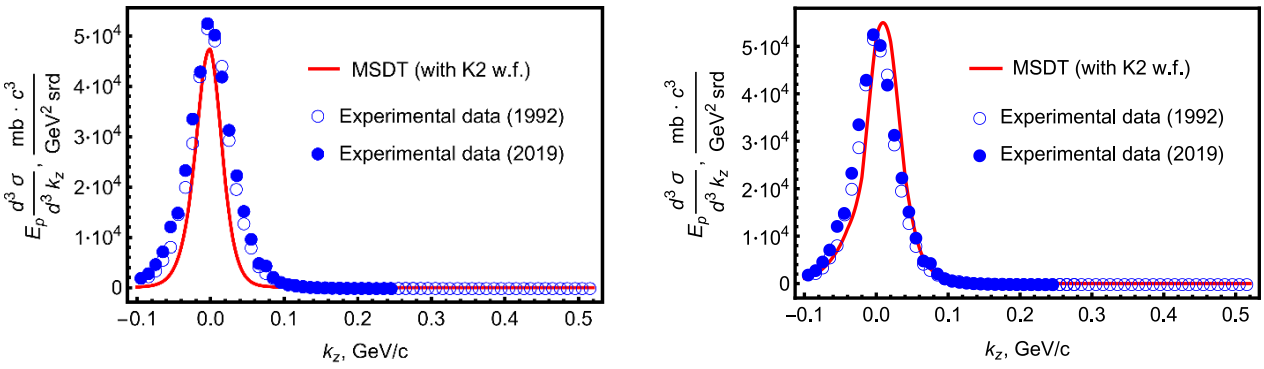

Fig. 3. *a* – $E_p \dfrac{d^3\sigma}{d^3k}$ vs k_z, using the multi-Gaussian K2 [43, 46] at $p_x = 10^{-5}$ GeV/*c*, $Q_z = 10^{-5}$ GeV/c.

b – The same $E_p \dfrac{d^3\sigma}{d^3k}$ vs k_z, at $p_x = 10^{-5}$ GeV/*c*, $Q_z = -0.05$ GeV/*c*. (See color Figure on the journal website.)

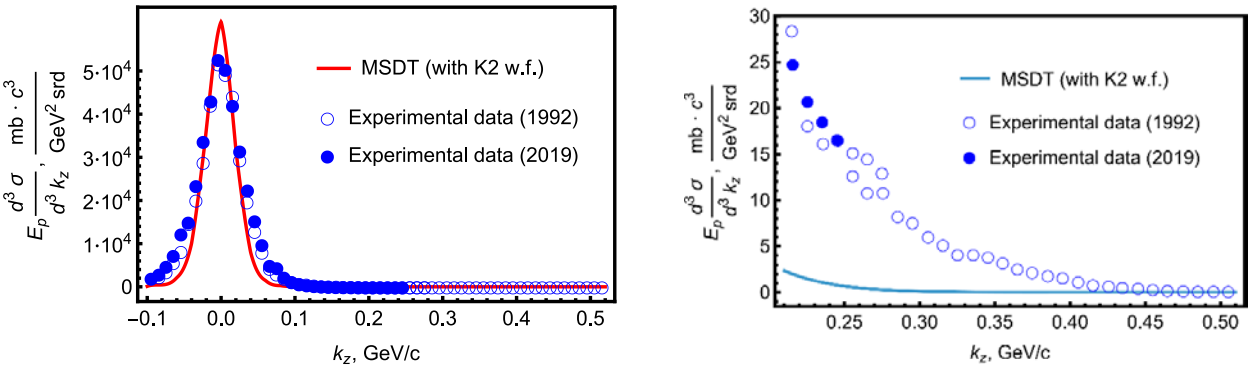

Fig. 4. *a* – The same as Fig. 3 at $p_x = 0.05$ GeV/*c*, $Q_z = 10^{-5}$ GeV/*c*. *b* – Within the MSDT model (K2 wave functions), dibaryons and possible *S*-quark states are not excluded in the region below $k_z = 0.40$ GeV/c ($p_x = 10^{-5}$ GeV/c, $Q_z = 0.015$ GeV/c). (See color Figure on the journal website.)

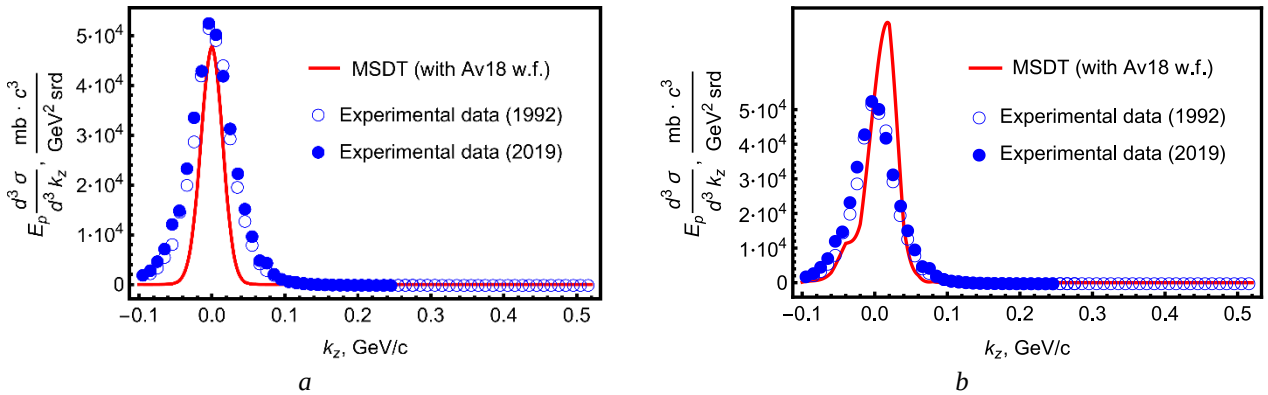

Fig. 5. *a* – $E_p \dfrac{d^3\sigma}{d^3k}$ vs k_z, using multi-Gaussian Av18 [44, 47] at $p_x = 10^{-5}$ GeV/c, $Q_z = 10^{-5}$ GeV/c.

b – The same $E_p \dfrac{d^3\sigma}{d^3k}$ vs k_z, at $p_x = 10^{-5}$ GeV/c, $Q_z = -0.05$ GeV/c. (See color Figure on the journal website.)

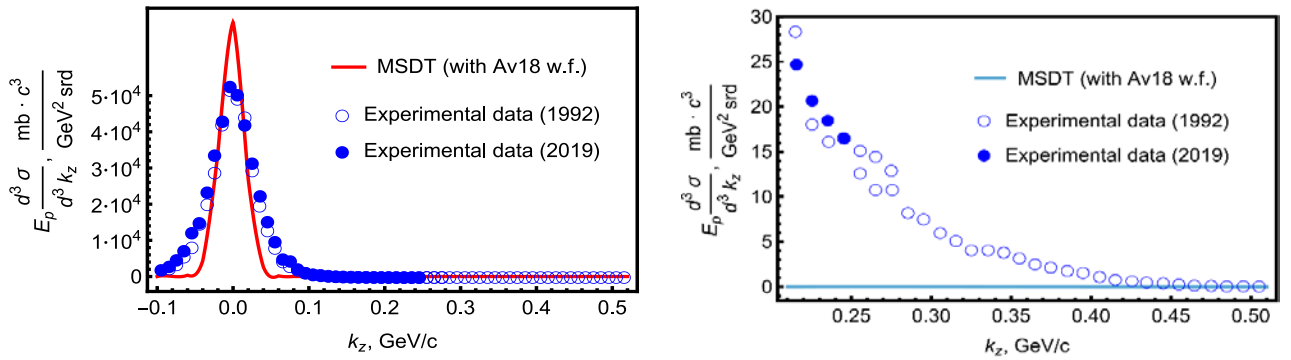

a *b*

Fig. 6. *a* – The same as Fig. 5 at p_x = 0.05 GeV/c, $Q_z = 10^{-5}$ GeV/c. *b* – Within the MSDT model (Av18 wave functions), dibaryons and possible *S*-quark states are not excluded in the region below k_z = 0.40 GeV/c ($p_x = 10^{-5}$-0.12 GeV/c, $Q_z = 10^{-5}$–0.5 GeV/c. (See color Figure on the journal website.)

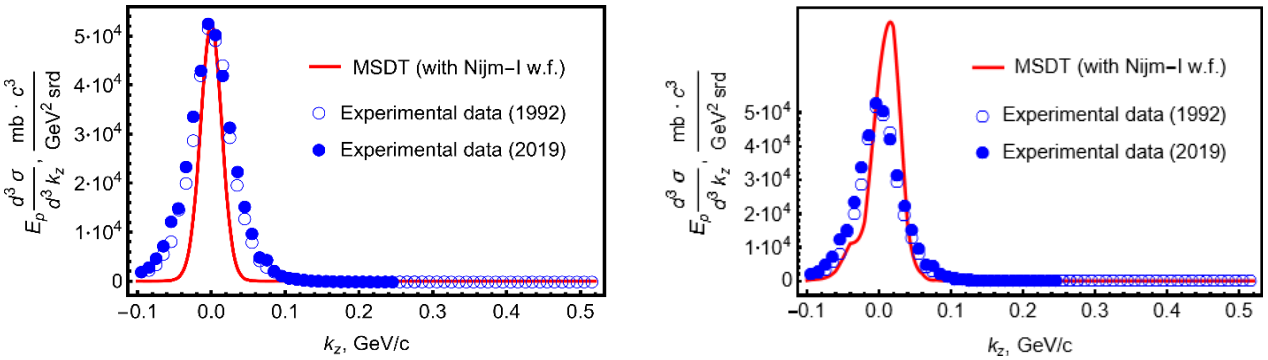

a *b*

Fig. 7. *A* – $E_p \frac{d^3\sigma}{d^3k}$ vs k_z, using multi-Gaussian Nijm I [36, 47] parametrization at $p_x = 10^{-5}$ GeV/c, $Q_z = 10^{-5}$ GeV/c.

b – The same $E_p \frac{d^3\sigma}{d^3k}$ vs k_z, at $p_x = 10^{-5}$ GeV/c, Q_z = –0.05 GeV/c. (See color Figure on the journal website.)

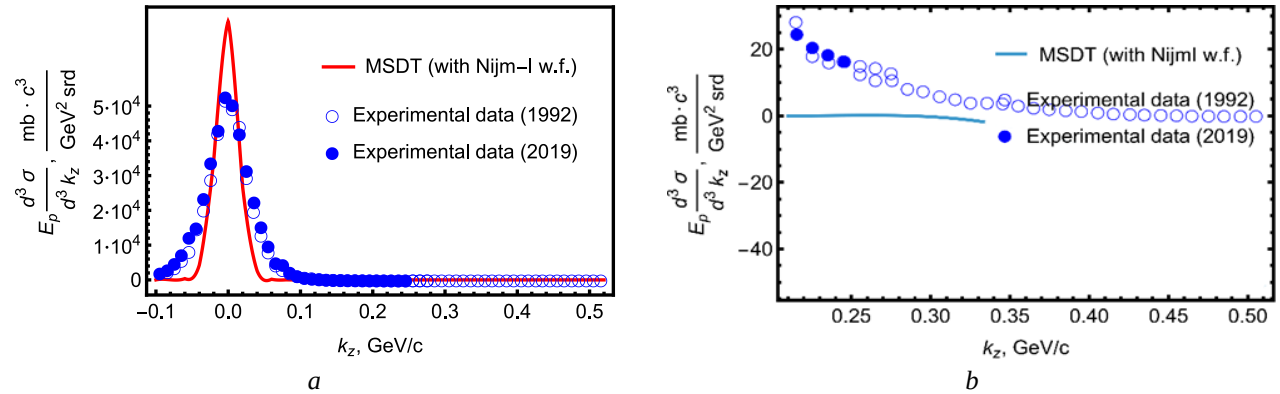

a *b*

Fig. 8. *a* – The same as Fig. 7 at p_x = 0.05 GeV/c, $Q_z = 10^{-5}$ GeV/c. *b* – Within the MSDT model with Nijm I, *d**(2380) is not excluded. Other dibaryons and possible *S*-quark states allowed below 0.5 GeV/c (p_x = 0.145 GeV/c, Q_z = −0.015 GeV/c, $N_s \to 0.94$). (See color Figure on the journal website.)

The MSDT parameters obtained based on the wave functions [33, 46, 47]

The model	Range parameter, Refs. [33, 46, 47]: $\lambda_i \left[\frac{1}{\text{fm}^2}\right]$	Cross-section: σ_N, mb	Slope parameter: β_N, fm	N_S, probabilities of the S-wave component
Gaussian	$\rightarrow 0.517$ (Ref. [33])	85	0.52	1
K2	$\rightarrow$ [46]	65	0.75	1
Av18	$\rightarrow$ [47]	45	1.25	1
Nijm I	$\rightarrow$ [47]	45	1.25	1(0.94)

Other parameters are presented in the Table. Parameters $M_d \rightarrow 1.87$ GeV/c and $\rho_N \rightarrow 1\cdot 10^{-3}$ are the same for all models.

5. Conclusion

Comparison with the experimental data (Figs. 1–8) show that the single-Gaussian model is inadequate and that an updated or alternative parameterization of the deuteron wave function is required. Small longitudinal momenta can account for the observed shift of the proton-yield maximum but do not significantly influence the dibaryon-like “enhancement” in the differential cross section.

Calculations within the Glauber - Sitenko framework using the K2, Av18, and Nijm I potentials do not confirm the existence of the dibaryon state $d^*(2380)$ (although the Nijm I potential leaves this possibility open). Nevertheless, other dibaryon-type resonances at lower momenta (0.23 - 0.4 GeV/c) and possible contributions from S-quark configurations cannot be excluded.

The enhancement observed in the 0.3 - 0.4 GeV/c region cannot be explained by multiple-scattering theory, supporting a quark-level interpretation rather than an explanation in terms of rescattered-pion contributions, in agreement with Refs. [7, 18, 20]. In the reaction $H(d, p)X$, the differential cross section increases with both the transverse momentum $\mathbf{p}_\perp$ and the magnitude of the longitudinal momentum transfer $|Q_z|$. A definitive assessment of the roles of Q_z and $\mathbf{p}_\perp$ requires inclusion of the corresponding Coulomb amplitudes in future calculations.

REFERENCES

1. M. Garcon, J.W. Van Orden. The Deuteron: Structure and Form Factors. In: J.W. Negele, E.W. Vogt (Eds.). *Advances in Nuclear Physics. Advances in the Physics of Particles and Nuclei*. Vol. 26. (Boston, MA, Springer, 2001) p. 293.
2. S. Amarasinghe et al. Variational study of two-nucleon systems with lattice QCD. Phys. Rev. D 107 (2023) 094508.
3. A.P. Kobushkin. Polarization observables in $A(d,p)$ breakup and quark degrees of freedom in the deuteron. Phys. Lett. B 421 (1998) 53; Phys. Atom. Nucl. 62 (1999) 1146; Yad. Fiz. 62 (1999) 1213.
4. M. Bashkanov, S.J. Brodsky, H. Clement. Novel six-quark hidden-color dibaryon states in QCD. Phys. Lett. B 727 (2013) 438.
5. L. Frankfurt, M. Strikman. Hard nuclear processes and microscopic nuclear structure. Phys. Rep. 160 (1988) 235.
6. Ya.D. Krivenko-Emetov, O.S. Shevchuk. Investigation of the internal structure of the deuteron against two-photon exchange effects in elastic electron-deuteron scattering. Nucl. Phys. At. Energy 25(4) (2024) 309.
7. V.G. Ableev et al. A study of the proton momentum spectrum from deuteron fragmentation at 8.9 GeV/c and an estimate of admixture parameters for the six-quark state in the deuteron. Nucl. Phys. A 393 (1983) 491; Nucl. Phys. A 411 (1984) 501; Sov. JETP Lett. 37 (1983) 196.
8. S.A. Zaporozhets et al. Study of high-energy deuteron interactions. Proceedings of the VIII International Seminar on High Energy Problems. Dubna, June 1986. JINR Report D1,2-86-668 (Dubna, 1986) p. 341.
9. C.F. Perdrisat et al. Cross section and T_{20} in 0° deuteron breakup at 2.1 GeV. Phys. Rev. Lett. 59 (1987) 2840.
10. V.G. Ableev et al. Tensor analyzing power of ^{12}C(d,p) at 9.1 GeV/c. Pis’ma v ZhETF 47 (1988) 558.
11. V. Punjabi et al. Deuteron breakup at 2.1 and 1.25 GeV. Phys. Rev. C 39 (1989) 608.
12. V.G. Ableev et al. Proton and triton momentum distributions from ^{4}He fragmentation at relativistic energies. JINR Rap. Comm. 5 (1990) 4; Few-Body Syst. 8 (1990) 137.
13. A.A. Nomofilov et al. Measurement of polarization transfer and the tensor analyzing power in polarized deuteron break-up with deuteron momenta up to 9 GeV/c. Phys. Lett. B 325 (1994) 327.
14. L.S. Azhgirey et al. Measurement of the tensor analyzing power T_{20} in inclusive deuteron breakup at

9 GeV/c on hydrogen and carbon. Phys. Lett. B 387 (1996) 37.
15. N.E. Cheung et al. Polarization transfer in ^{1}H(d,p)X at 2.1 GeV. Phys. Lett. B 284 (1992) 210.
16. B. Kuehn et al. The measurements of the polarization transfer coefficient in the (d, p) reaction at a fixed proton momentum 4.5 GeV/c and a deuteron momentum range of 6.0–9.0 GeV/c. Phys. Lett. B 334 (1994) 298.
17. T. Aono et al. Measurement of the tensor analyzing power T_{20} for $d^{\uparrow}$ + ^{12}C→p(0°)+X in the region of high internal momenta in the deuteron. Phys. Rev. Lett. 74 (1995) 4997.
18. A.P. Kobushkin, L. Vizireva. Relativistic polarised deuteron fragmentation into protons as a test of the six-quark nature of the deuteron at small distances. J. Phys. G 8 (1982) 893.
19. A.P. Ierusalimov, G.I. Lykasov, M. Viviani. Relativistic and spin effects in elastic backward p-d scattering. arXiv:1002.0249 (2010).
20. O.G. Sitenko, V.K. Tartakovskyi. *Nuclear Theory* (Kyiv: Lybid, 2000) 608 p. (Ukr)
21. M.N. Platonova. Dibaryon resonances and three-body forces in large-angle *pd* elastic scattering at intermediate energies. Phys. Part. Nucl. 54 (2023) 405.
22. P. Adlarson et al. Evidence for a new resonance from polarized neutron-proton scattering. Phys. Rev. Lett. 112 (2014) 202301.
23. V.G. Ableev et al. Momentum distribution of protons and deuterons from ^{3}He fragmentation by carbon at 10.78 GeV/c and zero angles. JETP Lett. 45 (1987) 596.
24. L.S. Azhgirey et al. Measurement of tensor analyzing power T_{20} in inclusive deuteron breakup at high energies. Phys. Atom. Nucl. 61 (1998) 432; L.S. Azhgirey et al. Tensor analyzing power T_{20} in backward elastic *dp* scattering and breakup at 0° between 3.5–6.5 GeV/c. Phys. Lett. B 391 (1997) 22.
25. J.S. Blair. Inelastic diffraction scattering. Phys. Rev. 115 (1959) 928.
26. A.I. Akhiezer, A.G. Sitenko. Diffractional scattering of fast deuterons by nuclei. Phys. Rev. 106 (1957) 1236.
27. O.F. Nemetz. On the high-energy scattering of deuterons by nuclei. Preprint. Institute for Nuclear Research, AS of UkrSSR. KINR-79-31R (Kyiv, 1980).
28. R.J. Glauber, G. Matthiae. High-energy scattering of protons by nuclei. Nucl. Phys. B 21 (1970) 135.
29. V.K. Tartakovsky, V.I. Kovalchuk. Disintegration of 23 and 26 MeV deuterons by ^{64}Cu and ^{197}Au nuclei. J. Phys. Stud. 10(1) (2006) 29. (Ukr)
30. V.K. Tartakovsky, O.I. Ivanova. The diffraction scattering of two-cluster nuclei on protons with taking into account the Coulomb interaction. Nucl. Phys. At. Energy 4(3) (2003) 44. (Ukr)
31. A.P. Kobushkin, Ya.D. Krivenko-Emetov. Effect of the Coulomb interaction in A(d,p) fragmentation. Ukr. J. Phys. 53 (2008) 751.
32. V.V. Davydovskyy, A.D. Foursat. Energy spectra of protons in diffraction break-up of deuterons on ^{12}C and ^{40}Ca at intermediate energies. Nucl. Phys. At. Energy 17(2) (2016) 111. (Rus)
33. V.K. Tartakovsky, A.V. Fursaev, B.I. Sidorenko. Diffractive dissociation of tritons by incident protons. Phys. Atom. Nucl. 68 (2005) 33.
34. I. Sitnik. Deuteron breakup at zero angle in the Coulomb nuclear field. EPJ Web Conf. 204 (2019) 10011.
35. Ya.D. Krivenko-Emetov. Effect of the Coulomb interaction to the processes of inelastic deuteron scattering on nuclei and the structure of deuteron. Manag. Dev. Complex Syst. 48 (2021) 75. (Ukr)
36. W.G.J. Stoks et al. Construction of high-quality *NN* potential models. Phys. Rev. C 49 (1994) 2950.
37. M.A. Braun, V.V. Vechernin. On the role of pion rescattering in the formation of cumulative protons from the deuteron. J. Exp. Theor. Phys. 40 (1984) 1588.
38. M.A. Braun, V.V. Vechernin. Contribution of pion rescattering to cumulative proton production on the deuteron. J. Exp. Theor. Phys. 43 (1986) 1579.
39. M. Buballa. NJL-model analysis of dense quark matter. Phys. Rept. 407 (2005) 205.
40. S. Gongyo et al. (The HAL QCD Collaboration). The d^*(2380) dibaryon from lattice QCD. Phys. Lett. B 811 (2020) 135935.
41. L.D. Landau, E.M. Lifshitz. *Quantum Mechanics. Non-Relativistic Theory*. 3rd ed. (Oxford: Pergamon Press, 1977) 688 p.
42. Ya.D. Krivenko-Emetov, B.I. Sidorenko. Inclusion of the longitudinal momentum-transfer component and kinematic factors in a diffraction approach for H(d,p)X reactions. arXiv:2508.06579 (2025).
43. D.V. Piatnytskyi, I.V. Simenog. Nuclear potentials for joint description of few-nucleon systems and structure functions of three-nucleon nuclei. Ukr. J. Phys. 53 (2008) 629; B.E. Grinyuk, I.V. Simenog. Precise variational calculations of energies and radii of D, T, ^{3}He, and ^{4}He nuclei. Ukr. J. Phys. 45 (2000) 21.
44. R.B. Wiringa, V.G.J. Stoks, R. Schiavilla. Accurate nucleon-nucleon potential with charge-independence breaking. Phys. Rev. C 51 (1995) 38.
45. M.V. Evlanov, A.D. Polozov, B.G. Struzhko. On the dependence of the differential cross-sections of deuteron break-up by atomic nuclei on the n-p potential form. Ukr. J. Phys. 25 (1980) 813.
46. L.A. Bulavin, V.I. Kovalchuk, A.V. Nosovskyi. *Scattering and Bound States in a System of Several Particles*. Monograph. (Kyiv: Institute for Safety Problems of NPPs, NAS of Ukraine, 2022) 200 p. (Ukr)
47. V.I. Zhaba. Wave Function and Polarization Characteristics of Processes Involving the Deuteron. Thesis for the degree of Candidate of Sciences in Physics and Mathematics (Uzhhorod: Uzhhorod National University; Institute for Nuclear Research, NAS of Ukraine, 2021) 135 p. (Ukr)

Я. Д. Кривенко-Еметов[1,2,3,*], Б. І. Сидоренко[2]

[1] *Національний технічний університет України «Київський політехнічний інститут імені Ігоря Сікорського», Київ, Україна*
[2] *Інститут ядерних досліджень НАН України, Київ, Україна*
[3] *Київський національний університет імені Тараса Шевченка, Київ, Україна*

*Відповідальний автор: y.kryvenko-emetov@kpi.ua; krivemet@ukr.net

ВРАХУВАННЯ ПОЗДОВЖНЬОЇ КОМПОНЕНТИ ПЕРЕДАНОГО ІМПУЛЬСУ Q_z ТА ПОПЕРЕЧНОГО ВІДНОСНОГО ІМПУЛЬСУ $\mathbf{p}_\perp$ У ДИФРАКЦІЙНОМУ ПІДХОДІ ДО РЕАКЦІЙ $H(d, p)X$

У рамках наближення Глаубера - Ситенка проаналізовано диференціальний переріз розпаду дейтрона з виходом протона при малих кутах (θ_p < 7 мкрад). Використано параметризації хвильової функції дейтрона: один гаусіан, а також моделі на основі NN-потенціалів K2, Av18 і Nijm I.

Досліджено вплив поздовжніх компонент імпульсу ($|Q_z| \le 0{,}5$ ГеВ/с) та поперечного імпульсу пари протон-нейтрон $(|\mathbf{p}_\perp| < 0{,}5$ ГеВ/с$)$ в антилабораторній системі. Результати порівняно з експериментом у діапазоні $k_z = p_3^* = 0{,}25 - 0{,}5$ ГеВ/с, де очікується прояв кваркових ефектів. Попередні оцінки показують збільшення перерізу зі зростанням $\mathbf{p}_\perp$ та зсув і посилення максимуму при врахуванні Q_z.

Ключові слова: дейтрон, дифракційний розпад, релятивістські ефекти, кваркова структура, переріз реакції, підхід Глаубера - Ситенка, антилабораторна система, поздовжній імпульс, поперечний імпульс, дибаріон, $d^*(2380)$.

Надійшла / Received 25.09.2025